Journal of Ceramic Processing Research. Vol. 17, No. 8, pp. 858~864 (2016)

J O U R N A L O F
Ceramic Processing Research

The microstructure evolution and mechanical properties of ammonium polyphosphate/ aluminium hydroxide/ mica during thermal reaction

Sheng HU[a,b], Fei Chen[a], Jun-Guo Li[a], Qiang Shen[a,*], Zhi-Xiong Huang[a] and Lian-Meng Zhang[a]

[a]*State Key Laboratory of Advanced Technology for Materials Synthesis and Processing, Wuhan University of Technology, Wuhan 430070, China*

[b]*School of Chemical and Environment Engineering, Hubei University for Nationalities, Enshi 445000, China*

The phase and microstructure evolution of ammonium polyphosphate/ aluminium hydroxide/ mica compounds (AAM) during thermal reaction are investigated. At 300 °C, AAM residues exhibit porous structure due to gas evolution from the thermal decomposition of ammonium polyphosphate (APP) and aluminium hydroxide, but mica does not react with them, and the flexural strength of specimens can reach 11.56 MPa. The thermal decomposition products of APP react with AlOOH to $NH_4AlP_2O_7$, which can improve the flexural strength during 300 ~ 400 °C. The reactivity of mica is increased by eliminating hydroxyl at temperature up to 600 °C, and the flexural strength of AAM residues is improved furtherly by the chemically interactions between active mica and phosphates during 600 ~ 1000 °C. And specifically at 1000 °C, the AAM residues exhibit relatively high flexural strength, which can reach 26.85 MPa and reactions between mica and $KAlP_2O_7$ could generate $KAlSi_3O_8$ and $3Al_2O_3{\cdot}2SiO_2$. AAM with high flexural strength from low to high temperatures is expected to be a kind of excellent inorganic additive of ceramifiable polymer with wide temperature range for using.

Key words: Ammonium polyphosphate, Mica, Aluminium hydroxide, Ceramifying process, Phase compositions, Microstructures, Mechanical properties.

Introduction

Ceramifying polymer composites ideally have the dual performance characteristics of polymers at room temperature and ceramics at elevated temperatures maintaining certain degree flexural strength, consisting of polymer matrix, mineral powder filler, structure control agent and other auxiliaries. Most studies of ceramifying composites have been carried out focussing on their excellent fireproofing [1-3]. Clay minerals can be used as an inorganic additive in ceramifying polymer, which will not only reinforce polymer, but also keep the shape of residues and improve the flame retardant effect in the ablation process [4-6]. Mica is a ratio of 2 : 1 layered aluminosilicate (ideal formula $KAl_2(Si_3Al)O_{10}(OH)_2$), one of the most popular fillers in polymer especially for flame retardant applications [7] and ceramifying polymer preparation [3], due to its high dielectric strength, high heat resistance and excellent corona resistance etc. It has been demonstrated that the addition of mica in ceramifying polymer sharply affects the structure and mechanical resistance of the ceramic like protective layer resulting in better fire retardant performance [2]. However, we have found that mica used as the only filler in silicone polymer showed low flexural strength at low-medium temperature, which can reach 0.3 MPa, 1.2 MPa and 2.2 MPa, respectively, after calcination at 600 °C, 800 °C and 1000 °C, respectively [6]. The flexural strength of ceramifying residue is improved by adding glass frits at low-medium temperature, after calcination at 600 °C, 800 °C and 1000 °C (0.88 MPa, 2.30 MPa and 3.53 MPa, respectively), due to the formation of more liquid phase that allows densification via liquid phase sintering from a eutectic reaction [8]. In the research for preparation of ceramifying polymer composites [2, 3, 7], silicone-based polymers have attracted considerable attention, such as silicon resin [7] and silicone rubber [8]. The ceramifying residue with good self-supporting is formed as a result from eutectic reactions at the interfaces between the mica particles and silica formed from decomposition of the silicone polymer matrix [8]. In the efforts to broad application of ceramifying polymer composites, polymer with non-silicone based become a trend for the ceramifying polymer composites preparation because of its low cost. Al-Hassany et al. reported the thermal reaction of binary inorganic mixtures (ammonium polyphosphate (APP)/$Al(OH)_3$, APP/$CaCO_3$, $CaCO_3$/$Al(OH)_3$, APP/mica) and ternary inorganic mixtures (APP/$CaCO_3$/mica and APP/$Al(OH)_3$/$CaCO_3$), which are believed to be the ceramifying additives in poly(vinyl acetate) with no silicone-based. Their results reveal that the ceramifying residue strength is the most prominently improved by introducting APP/$Al(OH)_3$ to the poly(vinyl

*Corresponding author:
Tel : +86-27-87217492
Fax: +86-27-87217492
E-mail: sqqf@263.net

acetate), which can reach 0.72 MPa after calcination at 400 °C [9].

The mechanism of ceramifying process of ceramifying polymer composites is the interactions in the inorganic substances essentially. However, the ceramifying process of polymer with no silicone-based is depend on the inorganic additives, because there is no residue involved in ceramifying process when fired at high temperature, especially, the phase compositions and microstructures evolution is essential to impvove the mechanical properties of ceramifying residues [9] and obtain good flame retardant properties [10]. For example, consequently investigations on the thermal degradation of APP/zinc borate mixtures have been carried out in order to explain that the combination of ammonium polyphosphate based compound and zinc borate in polypropylene leads to a synergistic effect in terms of fire behaviour [11]. With the incorporation of inorganic additive in ceramifying polymer composites, a significant improvement of the ceramifying behaviour is observed, but the understanding of their mode of action is not fully understood and it should be investigated. On the basis of the previous studies by Al-Hassany [9], the ammonium polyphosphate/ aluminium hydroxide/ mica compounds (AAM) with high flexural strength from low to high temperatures, is prepared by the combination of ceramifying of mica and synergistic flame retardance between ammonium polyphosphate and aluminium hydroxid in this paper. The mechanical properties is improved by phosphates [9,12,13] via reaction of ammonium polyphosphate and aluminium hydroxide in meso-low temperature (400 ~ 600 °C) and enhanced by the reactions in the phosphates and mica in high temperature.

Here, the phase compositions and microstructures evolution and mechanical properties of AAM with temperature increasing during thermal reaction process are studied using field emission scanning electron microscopy (FE-SEM) and X-ray diffraction (XRD), moreover ceramifying process and mechanism of AAM will be suggested. AAM is expected to be a kind of excellent inorganic additive of ceramifiable polymer with wide temperature range for using.

Experimental Procedures

Raw materials

Ammonium polyphosphate (APP) of commercial grade (crystalline form II, polymerization degree exceeds 1500) was supplied by Xingxing Fire-retardants Co., Ltd, Jiangsu, China. Aluminium hydroxide ($Al(OH)_3$) was from Sinopharm Chemical Reagent Co., Ltd, Shanghai, China. Mica was from Huayuan mica Co., Ltd, Hebei, China, with a mean particle size of 100 μm. The chemical compositions of the mica, determined by X-Ray Fluorescence (XRF), are given in Table 1.

Table 1. Chemical composition of mica.

Components	SiO_2	Al_2O_3	Fe_2O_3	MgO	CaO	Na_2O	K_2O
	49.97	27.30	5.32	1.12	0.037	0.46	9.85
wt%	TiO_2	P_2O_5	ZrO_2	Rb_2O	CeO_2	BaO	LOI
	0.79	0.026	0.045	0.024	0.075	0.028	4.82

Preparation of the ammonium polyphosphate/ aluminium hydroxide/ mica compounds (AAM)

A mixture of APP, $Al(OH)_3$ and mica compounds (AAM) were prepared with mass ratios of m_{APP}: $m_{Al(OH)3} : m_{mica} = 1 : 1 : 2$, by a high-speed mixer for 60 minutes, then put into the mold of Φ50 mm and compacted under 10 MPa pressure for 10 min to form green pellets. The obtained AAM green pellets were thermally heated from room temperature to target temperature at a heating rate of about 10 °C /min in a muffle furnace in air atmosphere. The solid residues were obtained when respectively heated to 300, 400, 600, 800, 1000 °C, holding for 60 min.

Characterization of the composites

Chemical compositions of mica were analyzed by the X-ray fluorescence method using a PANalytical B.V Axios advanced XRF spectrometer.

X-ray diffraction spectra of AAM after heat treatment were obtained using a Brucker AXS D8 X-ray diffractometer. Each scan was conducted from a 2θ angle of 5 ~ 55 ° at a scan rate of 4 ° /min.

After calcining, the apparent porosity of AAM residues was measured according to Archimedes displacement method using distilled water.

The residues of AAM were observed with field emission scanning electron microscope (Quanta-FEG250, FEI Co., USA) at an accelerating voltage of 20 kV. Samples were sputter-coated with gold using a Polaron Sputter coater unit.

Thermogravimetric analysis (TG) was performed on a thermogravimetric analyzer (STA449c/3/G, NETZSCH, Germany) at a heating rate of 10 °C /min (air atmosphere, flow rate of 50 ml/min). Samples were analyzed in the temperature range from 100 to 1000 °C. The calculated TG or DTG curves were summed up by the TG or DTG curves of the mixture ingredients weighted by their contents [14].

$$W_{cal}(T) = \sum_{i=1}^{n} x_i W_i(T) \quad (1)$$

where x_i is the content of compound i and W_i is DTG curve of compound i.

The flexural strength of pyrolysed samples was determined by the three-point bend method using an Instron Universal Testing Machine. Loading was applied using a cross-head speed of 0.5 mm/min. Samples measuring 40 mm × 4 mm × 3 mm were fired at various temperatures and held at the target temperature for 60 min. Typically between 8 and 10 samples were tested. The flexural strength was calculated using Eq.

$S = 3PL/(2bd^2)$, Where P is the maximumload (N), L the outer support span (mm), b the specimen width (mm) and d is the specimen thickness(mm), to give S in (MPa).

Results and Discussion

Thermal reaction behaviors of AAM

TG is one of the commonly used techniques in the evaluation of thermal stability, decomposition process and char residue of different materials. In order to understand the interactions in APP, $Al(OH)_3$ and mica, thermal degradation of APP, $Al(OH)_3$, mica and AAM are investigated by TG. The TG and DTG curves are shown in Fig. 1.

Fig. 1 reveals a distinctive difference in thermal decomposition behaviours of $Al(OH)_3$, APP, mica and AAM. During the degradation process of APP, it is clearly seen that the initial decomposition temperature of APP starts at 295 ºC and ends at 379 ºC, resulting in elimination of ammonia and water from APP to generate polyphosphoric acid [11]. The release of ammonia and water reaches the maximum value at 342 ºC. The gaseous degradation products release between 596 ºC and 693 ºC in the second step degradation process of APP are mainly composed of volatile P-O compounds [14], which is evolved from polyphosphoric acid decomposition. It can be seen that $Al(OH)_3$ undergoes three stages of thermal degradation process [15] at 227 ~ 260 ºC for the first stage and the second stage of 277 ~ 331 ºC, which are attributed to the elimination of water and then 471 ~ 561 ºC for the third stage resulting in elimination of water to generate Al_2O_3 [15], respectively. It can be seen that mica undergoes two stages of thermal degradation process at 97 ~ 164 ºC for the first stage which is attributed to the elimination of interlayer water and then 586 ~ 841 ºC for the second stage which is the dehydroxylation process of mica to generate lattice damage, vacancies and imperfection [16, 17], respectively, shown in Fig. 1.

Interactions in APP, $Al(OH)_3$ and mica can be revealed by comparing their experimental and calculated TG and DTG curves. The experimental and calculated TG and DTG curves of AAM are presented in Fig. 2. The thermal degradation behaviours of AAM is quite different from these of APP, $Al(OH)_3$, mica by showing only one main weight loss peak in the range of 229 ~ 319 ºC. The maximal peak at 292 ºC is mainly attributed to the thermal reaction between APP and $Al(OH)_3$. However, the thermal degradation process of AAM from calculated TG curves presented in Fig. 2 has already been described as a three steps degradation process at 227 ~ 329 ºC for the first step, the second step of 598 ~ 694 ºC and 775 ~ 865 ºC for the third step, respectively.

A comparison between the experimental and calculated TG curves of AAM is presented in Fig. 2. The difference

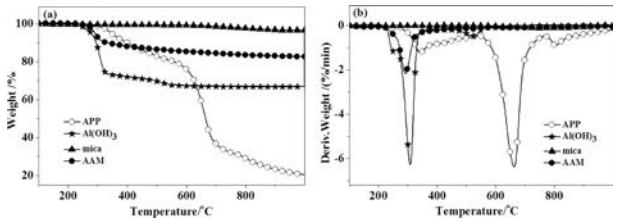

Fig. 1. TG(a) and DTG(b) curves of APP, $Al(OH)_3$, mica and AAM.

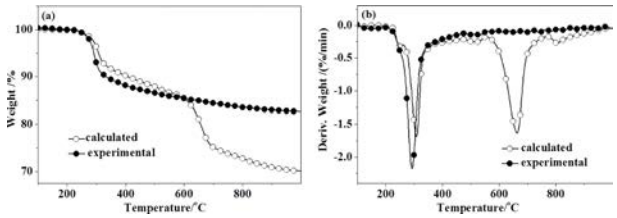

Fig. 2. Experimental and calculated TG(a) and DTG(b) curves of AAM.

between the two TG curves indicated a strong interaction in APP, $Al(OH)_3$ and mica. The AAM has similar TG behavior under the same conditions with a first decomposition step of $Al(OH)_3$ started at 227 ºC, explaining that only the decomposition of $Al(OH)_3$ happen and the addition of mica has no effect on the first decomposition step of $Al(OH)_3$. The mass loss rate of AAM at 292 ºC is much higher than the calculated mass loss rate at 309 ºC, meanwhile, the weight loss (9.2%) of AAM is more than the calculated weight loss (6.6%) between 229 ~ 319 ºC, indicating that reactions between APP and $Al(OH)_3$ could increase the weight loss of AAM. It can be seen that AAM undergoes only one stage of thermal degradation process without the second degradation step of 598 ~ 694 ºC and 775 ~ 865 ºC for the third degradation step from calculated TG curves of AAM principally corresponding to the degradation of APP, presented in Fig. 2, suggesting that APP is decomposed completely between 598 ~ 865 ºC in the thermal degradation process of AAM and a strong interaction in mica and thermal decomposition products of APP and $Al(OH)_3$ change decomposition of APP in the high temperature increasing the residues of AAM, which is beneficial to ceramifying.

Phase evolution of AAM during thermal reaction process

To explore further the changes in the thermal reaction after heat treatment at different calcined temperatures, the crystalline phases of the thermal reaction residues from AAM are analysed by XRD, presented in Fig. 3.

The XRD pattern for AAM at room temperature shows all peaks for the raw phase compositions of APP, $Al(OH)_3$ and mica. Fig. 3 shows that the new phases of AlOOH and $NH_4H_2PO_4$ are detected at 300 ºC suggesting that $Al(OH)_3$, APP decomposes to

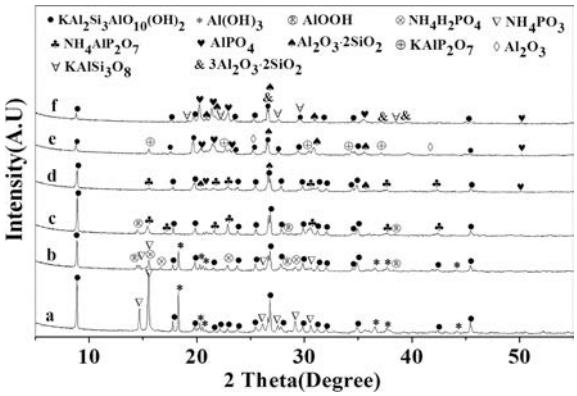

Fig. 3. The X-ray diffraction of residues of AAM with different decomposition temperatures. ((a) room temperature (25), (b) 300, (c) 400, (d) 600, (e) 800, (f) 1000).

AlOOH and $NH_4H_2PO_4$, respectively. In addition, mica do not react with the thermal decomposition products of $Al(OH)_3$ and APP. When heated to 400 ºC, APP, $Al(OH)_3$ and $NH_4H_2PO_4$ disappear showing that APP and $Al(OH)_3$ decompose completely. Moreover, mica and AlOOH are still detected, new phases of $NH_4AlP_2O_7$ are formed in the range of 300 ~ 400 ºC, suggesting that the thermal decomposition products of APP react with AlOOH to $NH_4AlP_2O_7$. Fig. 3 revealed that the new phases of $Al_2O_3·2SiO_2$ and $AlPO_4$ are formed at 600 ºC and mica and $NH_4AlP_2O_7$ are still detected, furthermore, AlOOH disappear suggesting that AlOOH decomposes completely and mica is involved in the reaction of the thermal decomposition products APP and $Al(OH)_3$. At temperature up to 800 ºC, mica, $Al_2O_3·2SiO_2$ and $AlPO_4$ are still detected but $NH_4AlP_2O_7$ is transformed into $KAlP_2O_7$ and AlOOH decomposes to Al_2O_3, as shown in Fig. 3. The formation of these compounds might then indicate the chemically interactions between active mica and phosphates, presented in Fig. 3. $KAlP_2O_7$ peaks are disappeared at 1000 ºC, which suggests that mica reacts with $KAlP_2O_7$ to form $KAlSi_3O_8$ and $3Al_2O_3·2SiO_2$.

These changes indicate that the reactions have taken place in APP, $Al(OH)_3$ and mica, resulting in the formation of phosphates at the meso-low temperatures (300 ~ 600 ºC) and aluminosilicate at high temperatures (800 ~ 1000 ºC), which might lead to strengthening the thermal reaction residues.

Proposed thermal reaction mechanism of AAM

According to the previous analyses of Fig. 1, Fig. 2 and Fig. 3, the thermal reaction process of AAM has a close correlation with the heating temperature. The thermal reaction of AAM can be divided into five stages: 25 ~ 300 ºC, 300 ~ 400 ºC, 400 ~ 600 ºC, 600 ~ 800 ºC, and 1000 ºC, according to the results of weight loss and mass loss rate of AAM, combined with the phase evolution of AAM after heat treatment at different calcined temperatures. The mechanism of thermal reaction of AAM might be described as follows.

First at about 227 ºC $Al(OH)_3$ decomposes to AlOOH and evolving water (first step of the TG curve of $Al(OH)_3$) (Eq. 2)), moreover, ammonium polyphosphate decomposes to yield polyphosphoric acid and evolving ammonia (Eq. 3), as it has been described in the literature[15] and [14], respectively.

$$AI(OH)_3 \rightarrow AIOOH + H_2O \uparrow \quad (2)$$

$$(NH_4)_{n+2}P_uO_{3n+1} + H_2O \rightarrow NH_4H_2PO_4 + (H_3PO_4) + NH_3 \uparrow \quad (3)$$

Between 300 and 400 ºC, polyphosphoric acid decomposes to polymetaphosphate and evolving water (Eq. 4), the polyphosphoric acid reacts with the AlOOH to form the char (pyrophosphate aluminium ammonium, $NH_4AlP_2O_7$ detected in the XRD) and release of water and ammonia the thermal reaction process occurs. (Eq. 5). In addition, in our case, the disappearance of $Al(OH)_3$ and $NH_4H_2PO_4$ might result from the decomposition of ammonium polyphosphate (Eq. 3) and $Al(OH)_3$ (Eq. 2) completely.

$$(H_3PO_4)_n \rightarrow (HPO_3)_n + H_2O \uparrow \quad (4)$$

$$NH_4H_2PO_4 + AIOOH + (H_3PO_4)_n \rightarrow NH_4AIP_2O_7 + H_2O \uparrow \quad (5)$$

Then according to our results, between 400 and 600 ºC, other reactions take place leading to the formation of $AlPO_4$ (Eq. 6) , $Al_2O_3·2SiO_2$ (Eq. 7) and other phases which has not been identified at this time (as explained in the XRD section). The formation of the γ-Al_2O_3 has been reported to be created during 400 ~ 600 ºC by Sato T resulting from direct degradation of AlOOH [15] (Eq. 8).

$$AIOOH + (H_3PO_4)_n \rightarrow AIPO_4 + H_2O \uparrow \quad (6)$$

$$AIOOH + (HPO_3)_n + NH_4AIP_2O_7 + KAI_2(Si_3AI)O_{10}(OH)_2 \rightarrow AIPO_4 + AI_2O_3·2SiO_2 + H_2O \uparrow + NH_3 \uparrow \quad (7)$$

$$AIOOH \rightarrow \gamma - AI_2O_3 + H_2O \quad (8)$$

Then the different analyses prove that a reaction in the degradation products of ammonium polyphosphate, pyrophosphate aluminium ammonium and mica occurs between 600 and 800 ºC leading to $Al_2O_3·2SiO_2$ and $KAlP_2O_7$. A possible way of formation of these compounds can be suggested (Eq. 9)). Moreover, á-Al_2O_3 which has been identified at this time can be suggested as indicated on Eq. 10.

$$(HPO_{3_n}) + NH_4AIP_2O_7 + KAI_2(Si_3AI)O_{10}(OH)_2 \rightarrow KAIP_2O_7 + AIPO_4 + AI_2O_3·2SiO_2 + H_2O \uparrow + NH_3 \uparrow \quad (9)$$

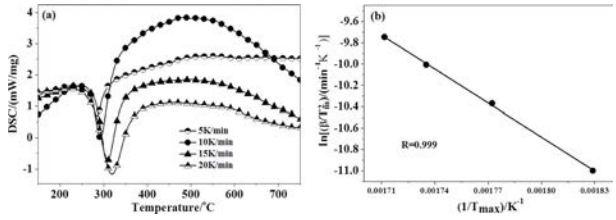

Fig. 4. DSC curves(a) and kissinger method applied to DSC data(b) for AAM at different heating rates.

$$\gamma-AI_2O_3 \rightarrow \alpha-AI_2O_3+H_2O\uparrow \quad (10)$$

It can be suggested that active mica reacts with the $Al_2O_3 \cdot 2SiO_2$ and $KAlP_2O_7$ to lead $KAlSi_3O_8$ and $3Al_2O_3 \cdot 2SiO_2$ at 1000 °C as described in the Eq. 11. The mechanisms exposed above explain the disappearing of $KAlP_2O_7$. The formation of $3Al_2O_3 \cdot 2SiO_2$ has been reported to be created by Lecomte GL. In our case, the formation of $3Al_2O_3 \cdot 2SiO_2$ and the disappearance of á-Al_2O_3 might result from the reaction, as it has been described in the literature [17] (Eq. 12).

$$AI_2O_3 \cdot 2SiO_2+KAIP_2O_7+KAI_2(Si_3AI)O_{10}(OH)_2 \rightarrow KAISi_3O_8+3AI_2O_3 \cdot 2SiO_2+H_2O\uparrow \quad (11)$$

$$AI_2O_3 \cdot 2SiO_2+AI_2O_3 \rightarrow 3AI_2O_3 \cdot 2SiO_2 \quad (12)$$

Kissinger method was used to calculate the apparent activation energy of the complex thermal reaction in APP, $Al(OH)_3$ and mica for analyzing and understanding the thermal reaction mechanism of AAM through reaction kinetics, which was obtained from relationship between the logarithms of β and the reciprocal of the absolute temperature at the maximum reaction rate. The Kissinger method adopts Eq. 13 [18]:

$$d[In(\beta/T_m^2)]/d(1/T_m) = -E_a/R \quad (13)$$

In this method, the involved usual symbols are summarized as follows:

E_a: apparent activation energies (kJ ·mol^{-1})

β: heating rate in the thermogravimetric analysis (K·min^{-1})

T_m: temperature at the inflection point of DTG curve

R: gas constant (8.3136 J·mol^{-1}·K^{-1})

The DTG curves of AAM with different heating rates (5 K/min, 10 K/min, 15 K/min and 20 K/min) under air atmosphere are shown in Fig. 4(a). The Kissinger method allows the determination of apparent activation energy without the knowledge of any thermal degradation reaction mechanism in advance. According to Equation (12), plots of $In(\beta/T_m^2)$ against $1/T_m$ produce the fitted straight lines as shown in Fig. 4(b). According to the slope of this straight line ($-E_a/R$), apparent activation energy E_a can be calculated and the apparent activation energy of AAM is 88.39 kJ / mol, less than the 121.16 kJ/mol which is the thermal decomposition reaction apparent activation energy of APP/mica in our previous study. The difference in the above apparent activation energies indicates that the thermal reaction apparent activation energy of AAM reduces and the thermal reaction rate of AAM increases with the addition of $Al(OH)_3$, which is helpful to generate ceramization residues for ceramifying.

Microstructure evolution of AAM during thermal reaction process

Observation of the cross-section structure of AAM residues revealed significant microstructural changes upon increasing the calcined temperature. The effect is demonstrated in Fig. 5. It can be seen that virtually loose structure occurs and the mica flakes are observed at room temperature, as seen from Fig. 5(a). A porous structure for a sample fired at 300 °C is observed, which should be gas evolution from the thermal

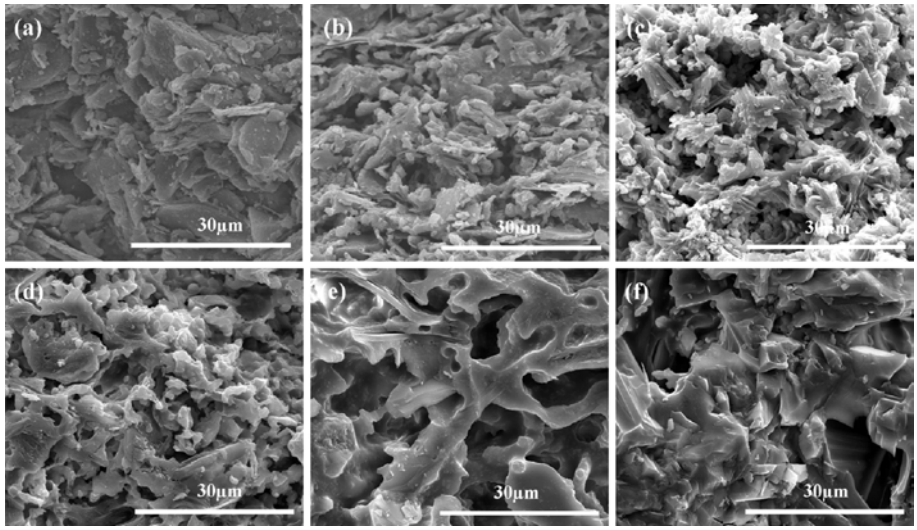

Fig. 5. FE-SEM images of AAM residues at different calcined temperatures. ((a) room temperature (25 °C), (b) 300 °C, (c) 400 °C, (d) 600 °C, (e) 800 °C, (f) 1000 °C).

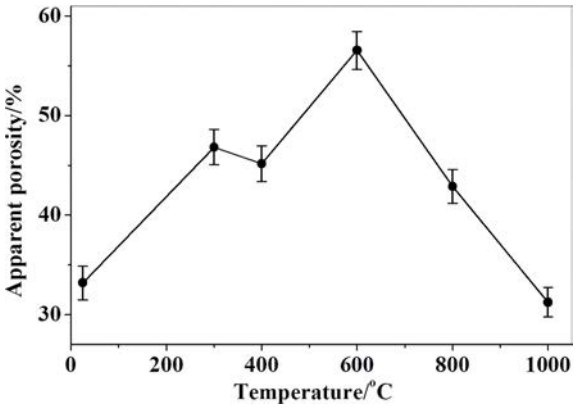

Fig. 6. The apparent porosity of AAM residues at different calcined temperatures.

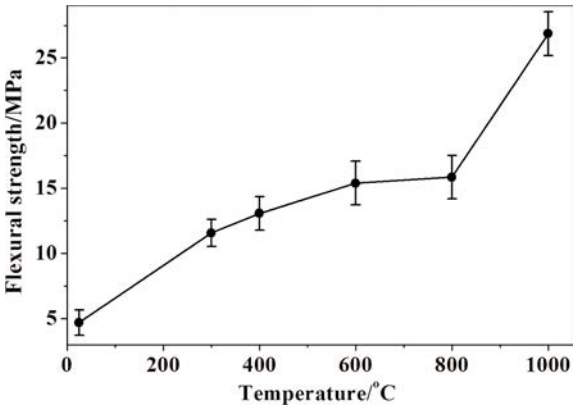

Fig. 7. The flexural strength of AAM residues at different calcined temperatures.

decomposition of APP and $Al(OH)_3$ at this temperature as mentioned by the analysis of Fig. 3. However, when the sample fired at 400 ºC, the reaction products act as a binder to form an adhesive surface layer, as observed in Fig. 5(c). The adhesive surface is strengthened by reactions between mica and phosphate in the range of 600 ~ 800 ºC, as shown in Fig. 5(d-e). The presence of significant ceramic grain indicate that coherent and dense microstructure occurs due to the reactions between mica and phosphates at 1000 ºC, which has the potential to improve the mechanical properties of the ceramic residues, presented in Fig. 5(f).

Fig. 6 shows the apparent porosity of AAM residues at different calcined temperatures. It is observed that with temperature increasing, the microstructure evolve accompanying with the phase evolution. From Fig. 6, it is obvious that apparent porosity of the AAM residues is in the range of 42.9% ~ 56.6%, due to gas evolution from the thermal reaction during 300 ~ 800 ºC, as shown in Fig. 6. Moreover, the microstructure study has shown that the ceramic residues heated at 1000 ºC has a coherent and dense layer reducing the apparent porosity to 31.2% and a porous structure, a combination which is anticipated to give satisfactory barrier characteristics for both heat and mass flow.

Mechanical properties evolution of AAM during thermal reaction process

Fig. 7 presents the flexural strength of the calcined specimens after heat treatment at various decomposition temperatures in air atmosphere. The flexural strength of AAM residues is dependent on phase composition and microstructural features, specifically calcined temperatures. In general, an increase in the flexural strength is observed with rising temperature. However, when temperature from 300 ºC to 800 ºC, a slowly increase in the flexural strength of the residue samples from 11.56 MPa to 15.85 MPa is due to the adhesive phosphate generated by the thermal reactions for improving the flexural strength but the porous structure hindering the rate of increasement. The specimens exhibit relatively high flexural strength, which can reach 26.85 MPa improved by the generation of ceramic residues to decrease the apparent porosity and form relatively dense structure when the calcined temperature is 1000 ºC. The flexural strength of ceramifying polymer composites is less than the AAM at various decomposition temperatures, due to no residue [9] or little residue [8] participation in ceramifying process from polymer pyrolysis.

Conclusions

In this work, the thermal reaction process of ammonium polyphosphate/ aluminium hydroxide/ mica compounds (AAM) has been investigated. The phase and microstructure evolution and mechanical properties of AAM during thermal reaction at different calcined temperatures are studied. It has been demonstrated that reactions occur between APP and $Al(OH)_3$ leading to the formation of aluminum phosphates which can improve the flexural strength during 300 ~ 600 ºC and the flexural strength of AAM residues is improved furtherly by the chemically interactions between active mica and phosphates during 600 ~ 1000 ºC. The different analyses have enabled to propose a detailed mechanism explaining the degradation and interactions of AAM. This study presents a practical interest in the ceramifying polymer field. It is expected to provide a kind of excellent inorganic additive of ceramifiable polymer with wide temperature range for using through the research of thermal reaction process of AAM.

Acknowledgments

The project is supported by the National Natural Science Foundation of China (No. 51472188, No.51521001) and “111” Project (B13035).

References

1. G. Alexander, Y.B. Cheng, R.P. Burford, J. Mansouri, C. Wood, K.W. Barber, P.D.D. Rodrigo and I. Ivanov, U.S.

Patent 7304245B2 (2007).
2. L.G. Hanu, G.P. Simon and Y.B. Cheng, Materials Science and Engineering A398 (2005) 180-187.
3. S. Hamdani, C. Longuet, D. Perrin, J.M. Lopez-cuesta and F. Ganachaud, Polymer Degradation and Stability 94[2] (2009) 465-495.
4. Y. Xia, X.G. Jian, J.F. Li, X.H. Wang and Y.Y. Xu, Polymer-plastics Technology and Engineering 46[3] (2007) 227-232.
5. M.A. Osman, A. Atallah, M. Müller, and U.W. Suter, Polymer 42 (2001) 6545-6556.
6. J. Mansouri, R.P. Burford and Y.B. Cheng, Materials Science and Engineering A 425[1] (2006) 7-14.
7. L.G. Hanu, G.P. Simon, J. Mansouri, R.P. Burford and Y.B. Cheng. Journal of Materials Processing Technology, 2004, 153-154(1): 401-407.
8. J. Mansouri, A. Chris, R. Katherine, Y.B. Cheng and R.P. Burford, Journal of Materials Science 42[15] (2007) 6046-6055.
9. Z. Al-Hassany, Ceramifiable Polymer Composites for Fire Protection Application, Thesis of RMIT University, 2007.
10. F. Samyn, S. Bourbigot, C. Jama, S. Bellayer, S. Nazare, R. Hull, A. Fina, A. Castrovinci and G. Camino. European polymer journal, 2008, 44(6):1631-1641.
11. F. Samyn, S. Bourbigot, S. Dequesne and R. Delobel, Thermochimica Acta 456 (2007) 134-144.
12. A. Castrovinci, G. Camino, C. Drevelle, S. Dequesne, C. Magniez and M. Vouters, European Polymer Journal 41 (2005) 2023-2033.
13. S.V. Levchik, G.F. Levchik, G. Camino and L. Costa, Journal of Fire Sciences, 13[1] (1995) 43-58.
14. W.Z. Jiang, J.W. Hao, Z.D. Han, Polymer Degradation and Stability 97[3] (2012) 632-637.
15. T. Sato, Thermochimica Acta 88[1] (1985) 69-84.
16. H.M. Zhou, X.C. Qiao, J.G. Yu. Applied Clay Science 80-81 (2013) 176-181.
17. G.L. Lecomte, J.P. Bonnet, P. Blanchart. Journal of Materials Science 42 (2007) 8745-8752.
18. H.E. Kissinger, Analytical Chemistry 29[11] (1957) 1702-1706.